# Thermodynamic and Kinetic Aspects of Lyotropic Solvation-Induced Transitions in Phosphatidylcholine and Phosphatidylethanolamine Assemblies Revealed by Humidity Titration Calorimetry

## H. Binder,*,† B. Kohlstrunk,‡ and W. Pohle§

*Institute of Medical Physics and Biophysics, University of Leipzig, Liebigstrasse 27, D-04103 Leipzig, Germany, Institute of Experimental Physics I, University of Leipzig, Linnèstrasse 5, D-04103 Leipzig, Germany, and Institute of Molecular Biology, Friedrich-Schiller-Universität Jena, Winzerlaer Strasse 10, D-07745 Jena, Germany*

Two selected unsaturated lipids, dioctadecadienoylphosphatidylcholine (DODPC) and dioleoylphosphatidylethanolamine (DOPE), undergo "solvation-induced" transitions at room temperature upon progressive hydration, varied via ambient relative humidity (RH), as demonstrated in the preceding first part of this study. These transitions are induced by the uptake of about one water molecule per lipid molecule in each case and change the lipid headgroups from a frozen, quasi-crystalline to a "melted" state. The partial molar enthalpy and partial molar entropy of water have been determined without significant interference of chain melting by a new adaptation of adsorption calorimetry, called humidity-titration calorimetry, coupled with gravimetry. The potency to form direct hydrogen bonds between the lipid headgroups decides whether the solvation-induced transition is exothermic (as in DODPC, no lipid−lipid H bonds) or endothermic (as in DOPE, lipid−lipid H bonds present). Consequently, the solvation-induced transition in DOPE is entropy-driven, and that in DODPC is enthalpy-driven. The time response of the calorimeter after a stepwise change of RH allows to study the kinetics of hydration with high resolution. In most cases, the response possesses exponential character. Despite several hypotheses that consider the adsorption process or diffusive transport of water, there is no straightforward interpretation of hydration kinetics so far. Hydration/dehydration hystereses were discussed in terms of metastability effects that accompany the formation of a complex structure in the headgroup region of the lipid aggregates.

## Introduction

This work is devoted to thermodynamic aspects of lyotropic phase transitions occurring in two selected unsaturated lipids, namely dioctadecadienoylphosphatidylcholine (DODPC) and dioleoylphosphatidylethanolamine (DOPE), structural aspects of which were studied in the preceding paper by using infrared spectroscopy.[1] These hydration-induced phase transitions, which comprise for DODPC two lamellar subgel phases ($SG_I$−$SG_{II}$) and for DOPE two nonlamellar fluid phases ($P_\alpha$−$H_{II}$), have in common to concern apparently only the polar region of the amphiphiles. Therefore, we have termed them solvation-induced transitions.

Recently, we developed a calorimetric technique called humidity-titration calorimetry (HTC), which directly measures the heat released/consumed upon adsorption/desorption of water onto/from amphiphiles after stepwise changes of the relative humidity, RH, in the sample cell of a mixing calorimeter.[2] It has been successfully applied to characterize lyotropic chain-melting transitions of amphiphiles enthalpically.[3] Used in conjunction with gravimetry, this method enables to determine the basic thermodynamic parameters owing to lipid hydration. Certainly, the thermodynamic characterization of the headgroup

region of the lipid assemblies represents one major prerequisite to understand important molecular aspects of membrane function. Using HTC and gravimetry, we will focus on determining thermodynamic and kinetic magnitudes related to water binding to PC and PE headgroups at the water activities that set going the solvation-induced transitions. Note that the solvation-induced transition proceeds without considerable changes of the structure of the hydrophobic core of the lipid aggregates. Therefore, we expect to obtain thermodynamic information without considerable interference from changes in the hydrophobic part of the lipids such as, e.g., chain melting. In most other cases lyotropic phase transitions involve the acyl chains and headgroups as well and thus it appears difficult to differentiate between effects due to the polar or apolar part of the lipids.

Phosphatidylcholines and phosphatidylethanolamines are well-known for exhibiting a number of systematic variations in relevant physical-chemical parameters, such as main-transition temperatures and aggregate morphology.[4−6] These variations have been attributed to the intrinsic property of these lipids to form basically different hydrogen-bonding patterns with predominantly lipid−water and lipid−lipid H bonds in their polar regions, respectively. It will be most intriguing to comparatively explore how these fundamental structural features affect the thermodynamic characteristics of the studied lipids, DODPC and DOPE.

From the RH−*T* phase diagrams determined in the accompanying paper, thermodynamic data that are independent

* To whom correspondence should be addressed. E-mail: binder@ rz.uni-leipzig.de. Fax: +49-341-9715709.
† Institute of Medical Physics and Biophysics, University of Leipzig.
‡ Institute of Experimental Physics I, University of Leipzig.
§ Friedrich-Schiller-Universität Jena.

**12050** *J. Phys. Chem. B, Vol. 104, No. 50, 2000*

Binder et al.
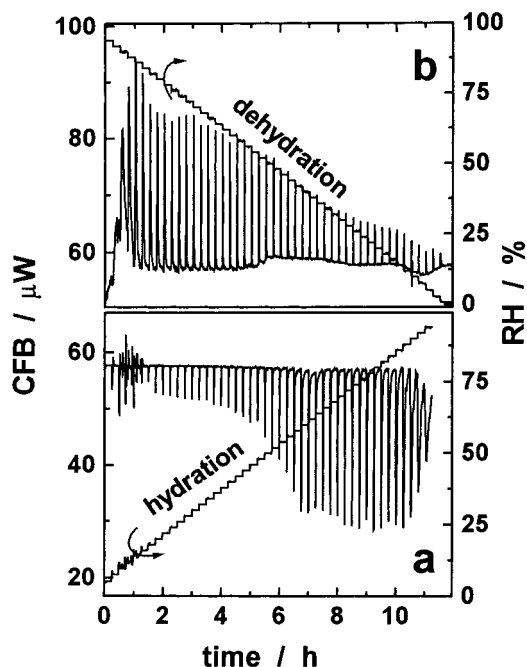


**Figure 1.** Raw data collected by a humidity titration experiment: The RH "staircase" (right axes) and the CFB pulses caused by the hydration (part a) and dehydration (part b) of 200 $\mu$g DOPE at $T = 25$ °C. The RH increment was $\Delta$RH = ±2%.



**Figure 2.** Measured heats of water adsorption, $q_{ITC}$, (part a, symbols) and molar ratios water per amphiphile, $R_{W/L}$ (part b, line), of DOPE at $T = 25$ °C as a function of the relative humidity, RH (hydration scan). The integrated heat of sorption, $Q_{ITC}$ (line in part a), and $R'_{W/L} = \partial R_{W/L}/\partial$RH (symbols in part b), are also shown.

of those obtained by HTC/gravimetry can be derived, thus giving the chance for judging the reliability of the latter. Besides yielding thermodynamic information, HTC measurements provide an access to kinetic data for lipid hydration. Here we present first results that illustrate both the potency and current problems of the method.

**Experimental Section**

**Materials.** For the preparation of lipid films we used stock solutions of the lipids DOPE (1,2-dioleoyl-sn-glycerophosphatidylethanolamine; from Sigma Co., Munich, Germany) and DODPC (1,2-bis(2-*trans*-4-*trans*-octadecadienoyl)-sn-glycerophosphatidylcholine; Nippon Oil and Fats Co., Japan) in methanol ($\sim$5−20 mM).

**Humidity Titration Calorimetry.** A detailed description of this new adaptation of classical adsorption calorimetry was given previously.[3,2] The essentials of the method can be summarized as follows. Definite volumes ($\sim$50 $\mu$L) of the stock solution were filled into the body of a cylindrical solid-particle-insert cell ($\sim$2 × 20 mm) of the MCS ITC calorimeter (MicroCal, Northampton, MA). The solvent was slowly evaporated under a stream of nitrogen by permanently rotating the cell. This procedure ensures the formation of a uniform film (mean thickness $\sim$1−5 $\mu$m) of the lipid ($\sim$50−200 $\mu$g) coating the inner wall of the cell.

The solid-particle-insert cell was mounted into the water-filled standard sample cell of the calorimeter. The insert cell was connected via a steel capillary and a thermostated tube to a moisture-regulating device (HumiVar, Leipzig, Germany) thus supplying a continuous flow of high-purity nitrogen gas of a definite relative humidity (RH) and temperature.[2,3] The gas flows through the access capillary into the cell, perfuses the sample film and leaves the cell through the outlet capillary to outside.

The RH of the $N_2$ gas was increased in steps of $\Delta$RH = 2% from 2% to 92% (hydration scan) or decreased in the opposite direction (dehydration scan) (see Figure 1 for illustration). The change of RH typically results in the adsorption/desorption of
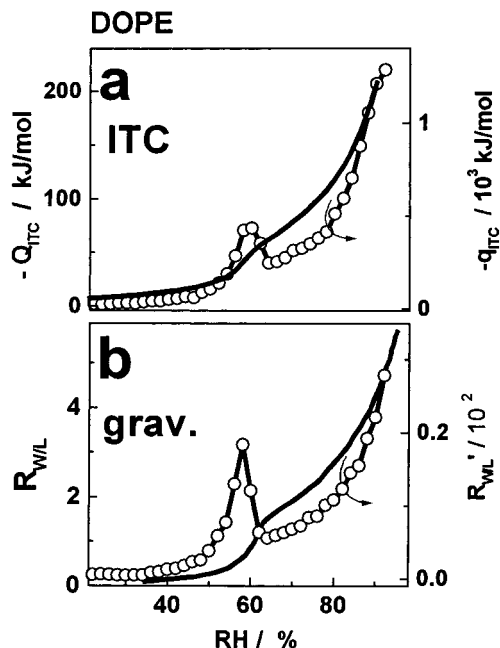
water onto/from the sample film. The corresponding heat of adsorption is detected as a power peak of the cell feedback circuit (CFB) of the calorimeter. The time interval between two subsequent RH steps ($\sim$15 min) was chosen to exceed the characteristic relaxation time of the system to ensure reequilibration after sorption (see also Figure 6). The baseline-corrected integral of the CFB peak at each RH step, $Q$, was normalized with respect to the amount of lipid in the sample cell, $N_L$ (moles), and the increment of water activity, $\Delta a_W = \Delta$RH/100%, to yield the observed heat $q_{ITC} = Q/(N_L \Delta a_W)$.

**Gravimetric Measurements.** The stock solution was spread on the surface of a circular quartz disk (diameter 15 mm) and allowed to dry under a stream of nitrogen. The sample was placed into a twin-microbalance system (Sartorius, Germany) equipped with a moisture-regulating device (see above and ref 7). Relative humidity was adjusted by flowing definitely moistened, high-purity $N_2$ gas through the sample chamber. Before the experiments were started, the lipid was dried for 12−24 h at RH = 0% until the mass of the sample attained a constant value ($\sim$0.5 mg). The mass increment due to water adsorption was recorded in the continuous mode by scanning RH with a constant rate of <±10%/h throughout the range of 0%−98%. The samples were investigated by means of increasing (hydration scan) as well as decreasing (dehydration scan) RH at constant temperature (25 °C) in analogy to the HTC experiments.

**Results**

**Isotherms and Heats of Water Adsorption.** Figure 1 depicts raw data typically obtained in the humidity-titration experiment with DOPE. Each RH jump causes a CFB pulse that is endothermic upon dehydrating and exothermic upon hydrating the sample. Integration of the pulses after baseline subtraction yields the heat, $q_{ITC}$, released (hydration) or consumed (dehydration) in each RH step as a function of the relative humidity, which is adjusted in the sample cell (see Figure 2a).

Thermodynamic and Kinetic Aspects of PC and PE Lipids

*J. Phys. Chem. B, Vol. 104, No. 50, 2000* **12051**

Part b of Figure 2 shows the results of the corresponding gravimetric experiment. The adsorption isotherm, $R_{W/L}(RH) = N_W/N_L$, gives the number of water molecules, $N_W$, sorbed onto $N_L$ lipid molecules as a function of RH. Its first derivative, $\partial R_{W/L}/\partial RH$, is proportional to the number of water molecules sorbed at the sample upon increasing RH. The heat of adsorption per mole of lipid, $q_{ITC}$, is related to $\partial R_{W/L}/\partial RH$ by[2,3]

$$q_{ITC} = 100\% \times \frac{\partial R_{W/L}}{\partial RH} \Delta h_w^{g \to s} \qquad (1)$$

where $\Delta h_w^{g \to s} \equiv h_w^s - h_w^g$ denotes the difference of the partial molar enthalpy of water in the sorbed and gaseous state. Note that the corresponding difference of the chemical potential is zero, i.e., $\Delta \mu_w^{g \to s} = 0$, because of thermodynamic equilibrium between gaseous and sorbed water.

The virtually parallel dependencies of $\partial R_{W/L}/\partial RH$ and of $q_{ITC}$ (cf. Figure 2) indicate that the shape of $q_{ITC}(RH)$ is mainly determined by $\partial R_{W/L}/\partial RH$ and only to a less extent by a change of the partial molar enthalpy of water upon adsorption, $\Delta h_W^{g \to s}$ (cf. eq 1). Both, $q_{ITC}$ and $\partial R_{W/L}/\partial RH$, show a pronounced peak in the medium range of RH. Accordingly, both the integrated number of adsorbed water molecules, $R_{W/L}$, and the integrated heat of adsorption

$$Q_{ITC}(a_W) \equiv \frac{1}{100\%} \int_0^{RH} q_{ITC} \, dRH \qquad (2)$$

exhibit a pronounced discontinuity at the corresponding water activity.

Interestingly, the adsorption characteristics of the PC closely resemble those of the PE. Both lipids only poorly adsorb water up to medium RH values. At a threshold value of RH, each of the DODPC and DOPE molecules imbibes $1-2$ water molecules. These findings can be clearly assigned to lyotropic phase transitions. As shown in the preceding paper, these events affect nearly exclusively the structure of the polar part of the lipids.[1] DOPE transforms from the ribbon ($P_\alpha$) phase into the inverse hexagonal ($H_{II}$) phase. DODPC undergoes a transition between two lamellar subgel phases, $SG_I$ and $SG_{II}$. The further enhancement of RH causes further, increasing adsorption of water.

Correlation plots between $Q_{ITC}$ and $R_{W/L}$ are shown in Figure 4. Note that the local slope equals $\Delta h_w^{g \to s}$ (cf. eqs 1 and 2). In the $P_\alpha - H_{II}$ phase transition range of DOPE $\Delta h_w^{g \to s}$ is significantly bigger (less negative) than in the $SG_I - SG_{II}$ phase transition range of DODPC.

**Kinetics of Water Adsorption.** Figure 5 depicts the mean equilibration time of water adsorption, $\tau_{eq} = t_{ads} - t_{blank}$, after each RH step. This has been estimated from the width of the CFB pulses, $t_{ads}$, and the time response of the calorimeter due to the gas exchange in the cell and the heat flow, $t_{blank} \approx 40$ s, which was measured in a blank experiment.[3] Note that the stepwise change of RH is considerably faster ($t_{step} \approx 15$ s) than $\tau_{eq}$. The mean decay time, $\tau_{eq}$, depends on the relative humidity in a similar fashion as $q_{ITC}$ (compare Figure 5 with Figures 2 and 3). Apparently, the observed heat varies with RH first of all due to kinetic effects and only to a less extend due to a change of the peak height. One can conclude that relaxation time is directly related to the slope of $R_{W/L}$, i.e., $\tau_{eq} \propto \partial R_{W/L}/\partial RH$. That means that the rate of water adsorption depends mainly on the number of water molecules adsorbed at a given RH. Note that $\tau_{eq}$ does virtually not depend on the gas-flow rate and on the amount of lipid if these parameters are varied by a factor of $0.5-2$.[3]
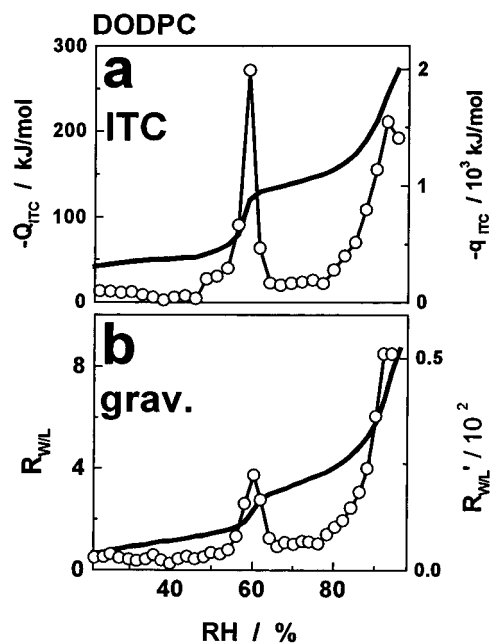


**Figure 3.** Measured heats, $q_{ITC}$, (part a, symbols) and molar ratio water per amphiphile, $R_{W/L}$ (part b, line), of DODPC at $T = 25$ °C as a function of relative humidity, RH (hydration scan). The integrated heat of sorption, $Q_{ITC}$ (line in part a), and $R'_{W/L} \propto \partial R_{W/L}/\partial RH$ (symbols in part b), are also shown.
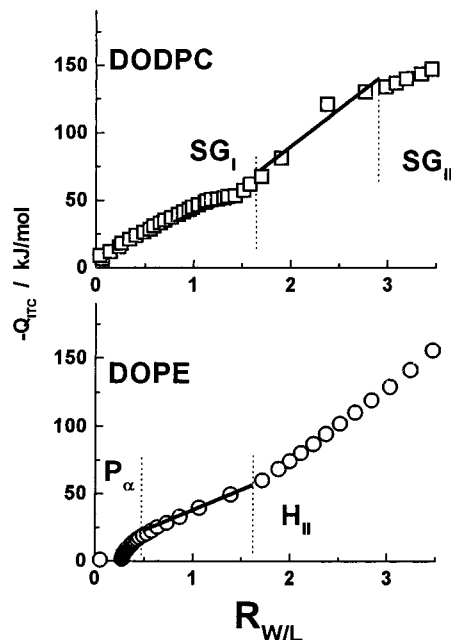


**Figure 4.** Correlation plots between $Q_{ITC}$ and $R_{W/L}$ for DODPC and DOPE (see also Figures 2 and 3). The phase transition ranges are indicated by vertical dotted lines. The slopes of the solid lines correspond to $\Delta h_w^{g \to s} = -30$ kJ/mol (DOPE) and $-55$ kJ/mol (DODPC).

The fast, stepwise change of RH allows a fairly detailed analysis of the kinetics of water adsorption. Figure 6 shows that both exponential and nonexponential decays of the heat responses occur.

## Discussion

**Partial Molar Enthalpy and Partial Molar Entropy of Water on Headgroup Solvation.** Combination of HTC and gravimetric measurements enables a thermodynamic character-
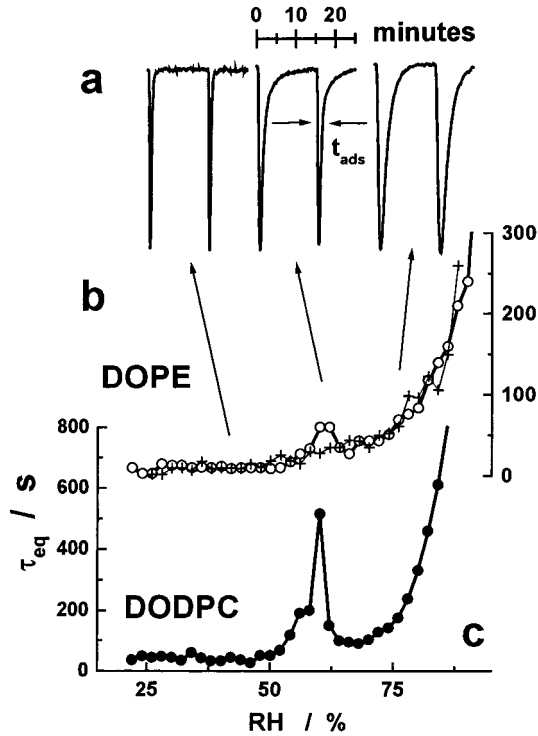
**Figure 5.** Kinetics of water adsorption onto DOPE and DODPC as a function of RH. Part a: Enlarged and normalized CFB peaks obtained by the HTC experiment of DOPE (cf. Figure 1, hydration scan) at different RH values (see arrows). Part b and c: Mean decay time of the CFB peaks, $\tau_{eq} = t_{ads} - t_{blank}$, as a function of RH. $t_{ads}$ is the width of the pulses at a height of $1/e$ of their maximum intensities. $t_{blank} = 40$ s denotes the width of the pulses of a blank experiment (see ref 3). The crosses in part b show the results of the corresponding dehydration experiment.
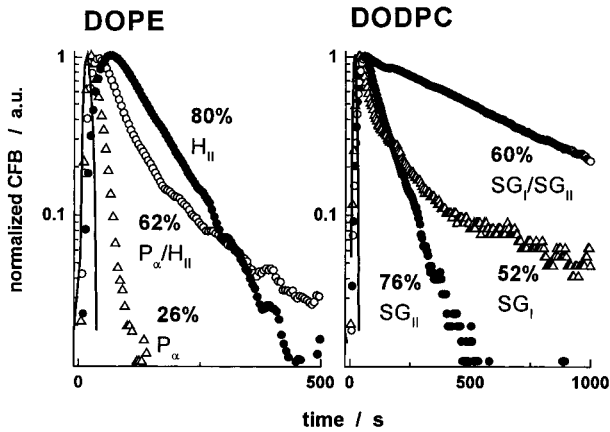


**Figure 6.** Semilogarithmic plots of selected heat pulses of DOPE and DODPC films obtained upon hydration. The RH values and the respective phases are given within the figure. The RH increment was 2%. The change of RH, $\partial RH/\partial t$, is shown by the solid lines.

ization of lipid hydration[2,3] and, in particular, of the headgroup-solvation-induced transitions of DOPE and DODPC. The samples can be considered as binary mixtures of lipid and water. The adsorption of water changes the composition of the system. The corresponding changes of the enthalpy, entropy and free enthalpy of the mixture, $H$, $S$ and $G$, respectively, are defined as the partial molar enthalpy, the partial molar entropy and the chemical potential (partial molar Gibbs free energy) of water, $h_W \equiv \partial H/\partial N_W$, $s_W \equiv \partial S/\partial N_W$ and $\mu_W \equiv \partial G/\partial N_W$, respectively. It appears appropriate to consider the difference of the thermo-

**TABLE 1: Thermodynamic Parameters for the Solvation of DOPE and DODPC ($T = 25$ °C)**

| lipid phase transition | DOPE $P_\alpha \rightarrow H_{II}$ | DODPC $SG_I \rightarrow SG_{II}$ |
|---|---|---|
| range of $R_{W/L}$ | 0.5−1.6 | 1.7−2.9 |
| $\Delta R_{W/L}$ | $1.1 \pm 0.2$ | $1.2 \pm 0.2$ |
| $a_W$ | $0.60 \pm 0.04$ | $0.58 \pm 0.04$ |
| $\Delta\mu_W^{b\rightarrow s}$/kJ/mol | $-1.3 \pm 0.2$ | $-1.3 \pm 0.2$ |

| lipid phase transition | HTC[a] | IR[b] | HTC[a] | IR[b] |
|---|---|---|---|---|
| $\Delta h_W^{b\rightarrow s}$/kJ/mol | $13 \pm 7$ | $4 \pm 4$ | $-10 \pm 7$ | $-9 \pm 4$ |
| $T\Delta s_W^{b\rightarrow s}$/kJ/mol | $14 \pm 7$ | $3 \pm 4$ | $-9 \pm 7$ | $-8 \pm 4$ |

[a] Determined from hydration scans carried out with HTC and gravimetry by means of eqs 4 and 5. [b] Determined from the temperature-dependent IR-measurements by means of eqs 6 and 7 (see accompanying paper[1]).

dynamic functions between sorbed and bulk (fluid) water, which is considered as reference state. For example,

$$\Delta\mu_W^{b\rightarrow s} \equiv \mu_W^s - \mu_W^b = RT \ln a_W \qquad (3)$$

gives the change of $\mu_W$ upon transfer of 1 mol water from the bulk to the sorbed state.[3] At thermodynamic equilibrium the water activity of sorbed water equals that of the vapor atmosphere in the sample chamber, $a_W = RH/100\%$. The experiments yield mean values (angular brackets) that correspond to a certain range of the water activity with the upper and lower limit, $a_W^2$ and $a_W^1$, respectively:

$$\langle \Delta h_W^{b\rightarrow s} \rangle = \frac{\Delta Q_{ITC}}{\Delta R_{W/L}} - \Delta h_W^{g\rightarrow b} \qquad \langle \Delta\mu_W^{b\rightarrow s} \rangle = \frac{\Delta G_{hyd}}{\Delta R_{W/L}}$$

$$T\langle \Delta s_W^{b\rightarrow s} \rangle = \langle \Delta h_W^{b\rightarrow s} \rangle - \langle \Delta\mu_W^{b\rightarrow s} \rangle \qquad (4)$$

with

$$\Delta Q_{ITC} = Q_{ITC}(a_W^2) - Q_{ITC}(a_W^1)$$

$$\Delta R_{W/L} = R_{W/L}(a_W^2) - R_{W/L}(a_W^2)$$

$$\Delta G_{hyd} = \int_{a_W^1}^{a_W^2} \Delta\mu_W^{b\rightarrow s} \frac{\partial R_{W/L}}{\partial a_W} da_W \qquad (5)$$

$\Delta h_W^{g\rightarrow b} = -44.6$ kJ/mol is the condensation heat of water. The results referring to the solvation-induced transition are given in Table 1. Note that a first-order phase transition is expected to proceed at one definite value of $a_W^{pt}$ where both phases co-exist. The width of the transition of $a_W^2 - a_W^1 \approx 0.03-0.06$ observed experimentally should be mainly attributed to meta-stability effects (vide infra).

Interestingly, the partial molar enthalpies of water adsorption at the solvation-induced transitions possess different signs for both investigated lipids. The adsorption of water onto the PC headgroups is exothermic whereas the adsorption of water to the PE headgroups is endothermic. Consequently, the solvation of the PE headgroups is driven by entropy giving rise to a more disordered state of the headgroups in the $H_{II}$ compared to the $P_\alpha$ phase as has been shown by IR spectroscopy. The physicochemical reason underlying this phenomenon is that the PE headgroups are involved into an energetically favorable network of H bonds before the solvation-induced transition. Hence, the incorporation of water between the headgroups and the partial replacement of headgroup-headgroup H bonds by water-

Thermodynamic and Kinetic Aspects of PC and PE Lipids

*J. Phys. Chem. B, Vol. 104, No. 50, 2000* **12053**

headgroup H bonds obviously weakens the intermolecular interactions on the average.

Contrarily, the PC groups are stabilized by relatively weak polar interactions in the almost dry state. Upon solvation they are replaced partially by stronger H bonds between water and lipid so that the system gains enthalpy. The decrease of entropy can be explained by the idea that the water in the first hydration shell of the lipid is more structured than with bulk water. IR linear-dichroism measurements reveal a high degree of molecular order of the sorbed water in the subgels of DODPC in agreement with this hypothesis.[8]

**Temperature Dependence of Lyotropic Phase Transitions.** The change of the Gibbs free energy at the boundary of the lyotropic phase transition (index "pt", note that here "$\delta$" refers to the difference between two phases and "$\Delta$" to the difference with respect to the reference state) is $\delta G^{i \to j} = \delta R_{W/L}^{i \to j} \mu_W^s|_{pt} = \delta H^{i \to j} - T_{pt}\delta S^{i \to j}$ (i, j = $P_\alpha$, $H_{II}$ or $SG_I$, $SG_{II}$).[3] Making use of $s_W^s|_{pt} \approx \delta S^{i \to j}/\delta R_{W/L}^{i \to j}$ and $h_W^s|_{pt} \approx \delta H^{i \to j}/\delta R_{W/L}^{i \to j}$, one obtains, after rearrangement and consideration of the reference state (bulk water),

$$\Delta\mu_W^{b \to s}\big|_{pt} = \Delta h_W^{b \to s}\big|_{pt} - T_{pt}\Delta s_W^{b \to s}\big|_{pt} \tag{6}$$

Differentiation yields the expression for the slope of the transition line in the $\Delta\mu^{b \to s} - T$ phase diagram

$$\frac{d\Delta\mu_W^{b \to s}}{dT}\bigg|_{pt} = -\Delta s_W^{b \to s}\bigg|_{pt} \tag{7}$$

Consequently, the slope of the transition line represents a measure of the partial molar entropy (and enthalpy) of the $\Delta R_{W/L}^{i \to j}$ water molecules that adsorb at the solvation-induced transition to each lipid (eqs 7 and 6).

The $\langle \Delta s_W^{b \to s} \rangle$ values determined by means of humidity-titration calorimetry and gravimetry predict a positive slope of the $SG_I$–$SG_{II}$ (DODPC) transition line, and a negative slope of the $P_\alpha$–$H_{II}$ (DOPE) transition line. In other words, the headgroup-melting transitions of both lipids are expected to shift on the RH scale into opposite directions with increasing temperature. The RH–$T$ phase diagrams of DOPE and DODPC have been determined by means of infrared spectroscopy (see accompanying paper[1]). As expected, the $P_\alpha$–$H_{II}$ transition of DOPE shifts to smaller and the $SG_I$–$SG_{II}$ transition of DODPC to bigger values of RH with increasing temperature. The slope of the respective transition line and eq 3 yield $\Delta s_W^{b \to pt}$ and $\Delta h_W^{b \to s}$ for a certain temperature ($T = 25$ °C), which are given in Table 1. The results of both independent methods (calorimetry/gravimetry and IR spectroscopy) agree within the error limits.

**Free Enthalpy of Dehydration.** With the special integration limits $a_w^1 = 1$ and $a_w^2 \equiv a_W$ eq 5 defines the free enthalpy of dehydration,

$$\Delta G_{dehyd} = \int_1^{a_W} \Delta\mu_W^{b \to s} \frac{\partial R_{W/L}}{\partial a_W} \, da_W$$

which gives a measure of the work to reduce the number of sorbed water molecules from $R_{W/L}(a_w^1 = 1)$ to $R_{W/L}(a_w^2 \equiv a_W)$.[9] A semilogarithmic plot of $G_{dehyd}$ as a function of $R_{W/L}$ yields a characteristic number of tightly bound water molecules, $R_{W/L}^0$, and the free enthalpy of complete dehydration, $\Delta G_0$, according to $\Delta G_{dehyd} = \Delta G_0 \exp(-R_{W/L}/R_{W/L}^0)$ (see Figure 7 and refs 3 and 10). Usually, it is more difficult to hydrate PE headgroups
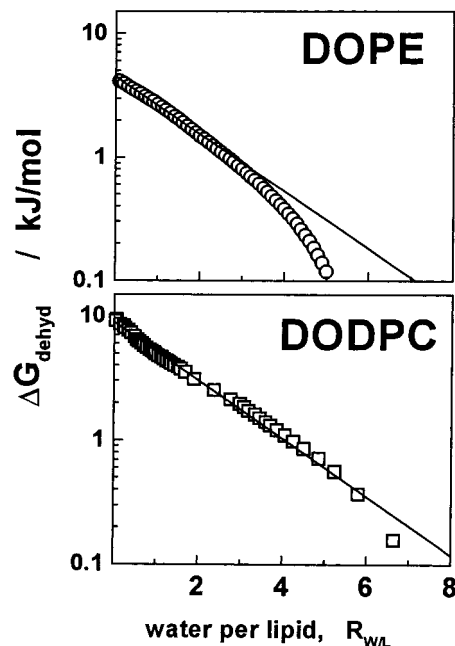
**Figure 7.** Semilogarithmic plots of the free energy of dehydration, $\Delta G_{dehyd}$, of DOPE and DODPC as a function of the number of water molecules per lipid, $R_{W/L}$. Lines are linear regressions yielding the number of tightly bound water molecules, $R_{W/L}^0$ and the free enthalpy of complete dehydration, $\Delta G_0$ according to $\Delta G_{dehyd} = \Delta G_0 \exp(-R_{W/L}/R_{W/L}^0)$.

than PC moieties. This leads to smaller values, $R_{W/L}^0(PE) \approx 1.8$ and $\Delta G_0(PE) \approx 6$ kJ/mol, when compared with those of common PC lipids, $R_{W/L}^0(PC) \approx 2.5-2.9$ and $\Delta G_0(PC) > 16$ kJ/mol.[11] The decay parameters of DOPE, $R_{W/L}^0(DOPE) = 1.85 \pm 0.05$ and $\Delta G_0(DOPE) = 4.5 \pm 0.5$ kJ/mol, agree with these values. Hence, the headgroups of DOPE appear to arrange and hydrate in a fashion characteristic of PE lipids. In contrast, the relatively small number of tightly bound water molecules of DODPC, $R_{W/L}^0(DODPC) = 1.85 \pm 0.05$, and the small free enthalpy of complete dehydration, $\Delta G_0(DODPC) = 9 \pm 1$ kJ/mol, indicates that the rigidization of the PC headgroups correlates with the dehydration of the lipid. In other words, DODPC membranes become more hydrophobic in the $SG_I$ phase than the membranes of other PC lipids.

**Hydration Kinetics.** The uptake of water by lipid films is significant in adsorption experiments to achieve equilibrium and for practical reasons for using lipid films in barrier or membrane applications. In general, the heat response of the calorimeter is expected to follow complex kinetics that involves different events such as water diffusion perpendicular and parallel to the polar interfaces, water binding to the polar groups of the lipid, changes of the aggregate structure on a molecular level and the heat transport to the wall of the calorimeter cell. The mean equilibration time, $\tau_{eq}$, was found to change in a similar way as the local slope of the adsorption isotherm, which gives a measure of the adsorption capacity at a particular RH value (Figure 5). On the other hand, the decay kinetics of heat pulses reveal either an exponential or a nonexponential behavior (Figure 6). Neither of the different decay laws observed can unequivocally assigned to a certain phase region, to the phase-transition ranges, or to the aggregates with frozen (DODPC) or fluid (DOPE) acyl chains. The distinct differences of the decay kinetics of one and the same lipid film indicates that the sorption rate of water, $dR_{W/L}/dt$, obviously dominates the heat response of the calorimeter. A considerable variation of the heat conductance of the different lipid films appears implausible.

**12054** *J. Phys. Chem. B, Vol. 104, No. 50, 2000*

Binder et al.

Recently, it was reported that the swelling kinetics of the lipid film in the calorimeter cell is limited by factors other than the water accessibility of the lipids at least in fluid phases.[2] Changes in the molecular packing are probably responsible for the relaxation rate. This hypothesis may explain that the hydration in the solid state of DODPC is slower in comparison to fluid DOPE and to both lipids at the solvation-induced transition. Possibly, the diffusive transport of water within films is responsible for the nonexponential decay kinetics in the crystalline $SG_I$ phase of DODPC. For the penetration of water through Langmuir–Blodgett films of crystalline fatty acids a vertical diffusion coefficient of $D_{\parallel} = 10^{-15}-10^{-11}$ m$^2$/s was estimated from their swelling kinetics in a humid atmosphere.[12,13] Accordingly, a water molecule would need a time of about $t \approx L^2/(4\pi D) = 10-10^4$ s for the transport parallel to the acyl chains considering a thickness of the lipid film of $L \approx 1$ $\mu$m. The leading term of the time function of diffusive water uptake is given by $dR_{W/L}/dt \propto t^{-0.5}$,[12] which results in a slowing down with increasing time in qualitative agreement with the observed decay behavior (Figure 6). A more detailed analysis of the curves however shows significant deviations of the hydration kinetics from a purely diffusive behavior in agreement with previous results.[12,14]

Other factors, such as several binding sites for water with different adsorption and desorption coefficients and/or several diffusive paths, e.g., through defects or pinholes,[14] can also account for the complex kinetics of water uptake in the $SG_I$ phase of DODPC. The nonexponential decay kinetics at the $P_\alpha$/$H_{II}$ phase transition of DOPE can be tentatively assigned to the complexity of the changes of the aggregate morphology, which are known to require longer equilibration times.

In most situations the water imbibes exponentially with time. The model of Langmuir adsorption predicts a first-order decay law of $dR_{W/L}/dt$ after a RH step (see Appendix, eq A4). The decay constant is however expected to increase linearly with $a_w = RH/100\%$ according to eq A3, in contrast to the results. The simple diffusion model (eq A5) suggests that the diffusion coefficient of water decreases proportional to $k_{eq}$ with increasing hydration. Such a behavior seems to be unrealistic because the mobility of water in the hydration shell of lipids remains constant or even increases with increasing distance from the headgroup and thus with $R_{W/L}$.[15] In summary, the slowing down of water uptake with increasing RH is not compatible with a purely diffusive mechanism and with the simple model of Langmuir adsorption.

Several effects of lipid hydration can be readily interpreted in terms of hydration pressure $\Pi = -\Delta\mu^{b\to s}/v_w$ ($v_w$ is the molar volume of water, $v_w = 1.8$ cm$^3$/mol).[16] The variation of the mean rate of hydration, $k_{eq} = \tau_{eq}^{-1}$, with RH can be analyzed in terms of an exponential function of the hydration pressure, which yields the activation volume of the process, $V_A$:

$$k_{eq} = k_{eq}^0 \exp\left(-\Pi \frac{V_A}{RT}\right) = k_{eq}^0 \exp\left(\Delta\mu^{b\to s} \frac{V_A}{RTv_w}\right) \quad (8)$$

From the slops of the semilogarithmic plots of $\ln k_{eq}$ versus $\Delta\mu^{b\to s}$ we obtained values of $V_A/v_w \approx 0$ before and of $-1.1 \pm 0.3$ (DOPE) and $-1.9 \pm 0.3$ (DODPC) after headgroup melting (not shown). The negative sign of $V_A$ reflects the decrease of the volume of the lipid–water systems with increasing $\Pi$ owing to the desorption of water. The absolute value of $V_A$ is comparable with the molar volume of water after the solvation-induced transition if the headgroups exist in a more disordered state. Contrarily, the rigid packing of the headgroups in the $P_\alpha$

and $SG_I$ phases appears to be largely independent of the very few water molecules that bind to the PE and PC moieties in the lipids studied here. Note that the exponential decay law (eq A4) remains valid because $k_{eq}$ is virtually a constant for a particular heat peak as the changes of the water activity used in the experiments ($\Delta a_w = 0.02$) are fairly small.

**Hysteresis Effects and the Hydrophobicity of the Surface.** Dependencies of relevant physical parameters on hydration and dehydration of both investigated lipids are characterized by a marked hystereses.[1,7,17] Those remain unchanged when the scans were slowed by a factor of 2. Recently, we showed that DODPC undergoes a highly cooperative transition from a metastable gel state into the subgel phase after an incubation time of several hours.[7,18] Metastability effects were mainly attributed to the crystallization of the acyl chains into a paraffin like packing motif. Pronounced hysteresis effects observed for ionic detergents upon chain freezing and melting confirm this interpretation.[3]

The hysteresis of DOPE should be essentially attributed to the polar region of the aggregates because the acyl chains remain in the fluid state before and after the $P_\alpha$/$H_{II}$ phase transition. Large hydration-dehydration hystereses of inorganic surfaces like silica were discussed in terms of wetting and unwetting phenomena.[19,20] Hydrophilicity and wetting of surfaces are the result of attractive forces between specific surface groups and water. In contrast, the weakening or the absence of these interactions makes a surface hydrophobic. For example, normally hydrophilic oxide surfaces can be hydrophobized by dehydroxylation, i.e., the substitution of water-surface (e.g., Si–OH·H$_2$O) by surface-surface (e.g., Si–O–Si) interactions.[20] The polar region of the DOPE aggregates changes its properties in a similar fashion upon transformation from the hydrated $H_{II}$ into the virtually dehydrated $P_\alpha$ phase. In this case, hydrogen bonds between headgroup and water (NH···OH$_2$ and PO···HOH) are replaced by direct H bonds between the headgroup (NH···OP). The corresponding dehydration proceeds at a smaller water activity than the restoration of the hydration shell. Note that the equilibration time, $\tau_{eq}$, is nearly equal for hydration and dehydration kinetics except the narrow range of the $P_\alpha \to H_{II}$ transformation (see Figure 5). Hence, the hysteresis is not the result of slowing down the desorption kinetics when compared with sorption process. Instead, it should be also attributed to metastability effects that accompany the formation of a complex structure in the headgroup region of the aggregates. Note that the dehydration of DODPC in the $SG_I$ phase also represents a sort of hydrophobization of the membrane.

### Summary and Conclusions

We have characterized the hydration of a phosphatidylethanolamine and of a phosphatidylcholine that undergo a lyotropic solvation-induced transition in the intermediate range of relative humidity at room temperature. Direct interactions between the lipid headgroups replace lipid–water interactions when going toward smaller values of water activity. As a result, the expenses of free energy to dehydrate the membrane decrease substantially. In addition, the headgroups lock into a highly ordered structure.[1] The ability to form direct hydrogen bonds between the headgroups decides whether the solvation-induced transition is accompanied by a gain (no H bonds, PC) or loss (H bonds, PE) of enthalpy. Thus, it is the intrinsic "chemical" nature of the surface that predominantly accounts for the essentials of lipid hydration. These results illustrate the structural and thermodynamic background of hydrophobization phenomena of surfaces that are known to promote the aggregation and fusion of biological membranes.

Thermodynamic and Kinetic Aspects of PC and PE Lipids

*J. Phys. Chem. B, Vol. 104, No. 50, 2000* **12055**

White and Whimley demonstrated the diagnostic power of a whole-residue hydrophobicity scale of amino acids to predict the affinity of polypeptides to lipid membranes.[21] There exist pronounced differences between hydrophobicity scales based either on *n*-octanol/water or on lipid membranes/water partitioning probably because of the complex nature of the interfacial region that cannot be simply specified by a single parameter. The ability to form hydrogen bonds seems to play an important role for several residues that prefer the interfacial region of the membrane as has been demonstrated, for example, for the incorporation mode of cholesterol into PC membranes.[22] In this sense, the nature of lipid headgroups may be the rationale to govern the partitioning behavior and, thus, to modulate the biological activity of additives.

The slopes of the transition lines of temperature/hydration phase diagrams yield the partial molar entropies of water binding at the solvation-induced transition. The potential of humidity titration calorimetry to characterize lyotropic phase transitions enthalpically has been demonstrated. Moreover, this method allows to study the kinetics of adsorption processes with high resolution at any value of water activity, making this method superior to the approaches in other dynamic hydration experiments.[12,23-25] However, the kinetics of spontaneous hydration resulting from large changes of water activity should be interpreted with care because of the hydration dependence of kinetic parameters and possible metastability effects. A sound kinetic model should explain the time dependence of adsorption and the variation of the kinetic parameters with water activity of as well. Despite several hypotheses, there is no satisfactory interpretation of the kinetics of hydration/dehydration and of the observed hysteresis effects. A combination of time-dependent IR-spectroscopic, gravimetric and calorimetric experiments would possibly enable a considerable progress of this issue.

## Appendix

**Exponential Models of Adsorption Kinetics.** The model of Langmuir adsorption assumes that in the case of incomplete hydration a maximum number of adsorption sites, $R_{W/L}^{max}$, splits into free and occupied ones ($R_{W/L}^{max} - R_{W/L}$ and $R_{W/L}$, respectively). The kinetic balance of adsorption and desorption gives rise to the differential equation

$$dR_{W/L}/dt = k_+ a_W (R_{W/L}^{max} - R_{W/L}) - k_- R_{W/L} \qquad (A1)$$

where $k_+$ and $k_-$ denote the respective rate coefficients. Note that the sorption rate depends on the partial pressure of the sorbate in the gas phase and thus on $a_W$. The solution of eq A1 can be written in the form

$$R_{W/L}(t) = R_{W/L}(\infty) - \{R_{W/L}(\infty) - R_{W/L}(0)\} \exp(-k_{eq}t) \quad (A2)$$

where $R_{W/L}(0)$ and $R_{W/L}(\infty)$ are the $R_{W/L}$ values before and after an infinitely fast RH step at $t = 0$ and at $t = \infty$, respectively. The difference becomes $\{R_{W/L}(\infty) - R_{W/L}(0)\} \approx \Delta a_W \partial R_{W/L}/$

$\partial a_W$ at small increments of the water activity, $\Delta a_W$. The decay constant is given by

$$k_{eq} = k_+ a_W + k_- \qquad (A3)$$

The time-dependent rate of sorption obeys also the exponential law

$$dR_{W/L}/dt = \Delta a_W \partial R_{W/L}/\partial a_W' k_{eq} \exp(-k_{eq}t) \qquad (A4)$$

The real situation of water uptake of a multilayered lipid film is, however, more complicated because of additional effects such as (i) there are different water-binding sites with different sorption and desorption coefficients, (ii) the transport of water from the upper boundary into the bulk of the film is diffusive, and (iii) there is coupling between water binding and changes of the molecular structure and aggregate morphology. Effect (i) can be formally taken into account if one writes $k_{eq}$ as a function of $R_{W/L}$, $k_{eq}(R_{W/L})$ (vide supra). The exponential laws according to eqs A2 and A4 remain valid at small steps of $\Delta a_w$ (and $\Delta R_{W/L}$). A simple treatment of water diffusion (ii) yields exponential kinetics similar to that of eqs A2 and A4 with

$$k_{eq} = GD/L^2 \qquad (A5)$$

where $G$, $D$, and $L$ denote a geometric factor, the diffusion coefficient and the thickness of the film, respectively.[25]

### References and Notes

(1) Binder, H.; Pohle, W. *J. Phys. Chem. B* **2000**, *104*, 12039.

(2) Binder, H.; Kohlstrunk, B.; Heerklotz, H. H. *Chem. Phys. Lett.* **1999**, *304*, 329.

(3) Binder, H.; Kohlstrunk, B.; Heerklotz, H. H. *J. Colloid Interface Sci.* **1999**, *220*, 235.

(4) McIntosh, T. J. *Biophys. J.* **1980**, *29*, 237.

(5) Tate, M. W.; Gruner, S. M. *Biochemistry* **1989**, *28*, 4245.

(6) Cevc, G. *Biochemistry* **1987**, *26*, 6305.

(7) Binder, H.; Anikin, A.; Kohlstrunk, B.; Klose, G. *J. Phys. Chem. B* **1997**, *101*, 6618.

(8) Binder, H.; Gutberlet, T.; Anikin, A.; Klose, G. *Biophys. J.* **1998**, *74*, 1908.

(9) Cevc, G. J. *Chem. Soc.*, *Faraday Trans.* **1991**, *97*, 2733.

(10) Rand, R. P.; Parsegian, V. A. *Biochim. Biophys. Acta* **1989**, *988*, 351.

(11) Binder, H.; Dietrich, U.; Schalke, M.; Pfeiffer, H. *Langmuir* **1999**, *15*, 4857.

(12) Girard, K. P.; Quinn, J. A.; Vanderlick, T. K. *J. Colloid Interface Sci.* **1999**, *217*, 146.

(13) Ariga, K.; Okahata, Y. *Langmuir* **1994**, *10*, 3255.

(14) Marshbanks, T. L.; Ahn, D. J.; Franses, E. I. *Langmuir* **1994**, *10*, 276.

(15) Klose, G.; Arnold, K.; Peinel, G.; Binder, H.; Gawrisch, K. *Colloids Surf.* **1985**, *14*, 21.

(16) Parsegian, V. A.; Fuller, N.; Rand, R. P. *Proc. Natl. Acad. Sci. U.S.A.* **1979**, *76*, 2750.

(17) Selle, C.; Pohle, W.; Fritzsche, H. *J. Mol. Struct.* **1999**, *480-485*, 401.

(18) Binder, H.; Kohlstrunk, B. *Vibr. Spectrosc.* **1999**, *21*, 75.

(19) Inagaki, S.; Fukushima, Y.; Kuroda, K.; Kuroda, K. *J. Colloid Interface Sci.* **1996**, *180*, 623.

(20) Feng, A.; McCoy, B. J.; Munir, Z. A.; Cagliostro, D. E. *J. Colloid Interface Sci.* **1996**, *180*, 276.

(21) White, S. H.; Wimley, W. C. *Biochim. Biophys. Acta* **1998**, *1376*, 339.

(22) Pasenkiewicz-Gierula, M.; Rog, T.; Kitamure, K.; Kusumi, A. *Biophys. J.* **2000**, *78*, 1376.

(23) Pohle, W.; Selle, C.; Fritzsche, H.; Binder, H. *Biospectroscopy* **1998**, *4*, 267.

(24) Wadsö, I.; Wadsö, J. *J. Therm. Anal.* **1997**, *49*, 1045.

(25) Lovell, M. R.; Roser, S. J. *Langmuir* **1996**, *12*, 2764.